Seasonal to interannual variability of the eddy field in the Labrador Sea from satellite altimetry

Peter Brandt, Friedrich A. Schott, Andreas Funk, and Carlos S. Martins
Institut für Meereskunde, Universität Kiel, Kiel, Germany

Received 19 July 2002; revised 6 February 2003; accepted 18 December 2003; published 27 February 2004.

[1] Sea level anomalies measured by the altimeters aboard the TOPEX/Poseidon and ERS satellites for the periods 1993–2001 and 1997–2001, respectively, are used to investigate the eddy field in the subpolar North Atlantic and in the Labrador Sea. A quadratic correction of the obtained eddy kinetic energy (EKE) with respect to significant wave height is applied that led to an increased correlation between moored and altimetric EKE in the central Labrador Sea. The mean EKE field shows higher levels associated with the main currents and a strong seasonality in the Labrador Sea. The annual cycle of the EKE shows a propagation of West Greenland Current (WGC) EKE into the central Labrador Sea with a mean southward propagation speed of about 3 cm s^{-1}, while the EKE maximum in the Labrador Current is well separated from the interior by local EKE minima. The interannual variability of the EKE in the Labrador Sea shows distinct regional differences. In the WGC region, strong early winter maxima are found during 1993 and 1997–1999. In the central Labrador Sea, maxima are found during March/April 1993–1995 and 1997. Variations in the annual cycle of the WGC EKE are observed: While there is a weak annual cycle in the WGC region during 1994–1996 with more continuous EKE generation, during 1997–2000, there is a strong seasonal cycle with maximum EKE during January and particularly low EKE during summer. The propagation of WGC EKE into the central Labrador Sea is enhanced during 1997–2000, leading to a long persistence of EKE in the central Labrador Sea. During 1993–1995 and 1997 the central Labrador Sea EKE almost instantaneously increased during March/April, followed, in the earlier years, by a relatively fast destruction of the winterly generated EKE. *INDEX TERMS:* 4207 Oceanography: General: Arctic and Antarctic oceanography; 4215 Oceanography: General: Climate and interannual variability (3309); 4520 Oceanography: Physical: Eddies and mesoscale processes; *KEYWORDS:* Labrador Sea, eddy kinetic energy, altimetry

Citation: Brandt, P., F. A. Schott, A. Funk, and C. S. Martins (2004), Seasonal to interannual variability of the eddy field in the Labrador Sea from satellite altimetry, *J. Geophys. Res.*, *109*, C02028, doi:10.1029/2002JC001551.

1. Introduction

[2] The Labrador Sea is a region of great interest because of its role in water mass formation, thermohaline circulation, and possibly climate change. It is one of the few sites of the world ocean where open ocean convection occurs, occasionally reaching great depths. Open ocean convection sites are characterized by a cyclonic circulation, weak stratification in the interior, and the associated rising of isopycnals in the center [*Marshall and Schott*, 1999]. The cyclonic gyre in the Labrador Sea includes the West Greenland Current (WGC) flowing northwestward and the Labrador Current (LC) which flows southeastward. The WGC is mainly fed by the East Greenland Current (EGC) that involves two branches: the classical shallow EGC branch over the shelf with colder temperatures, and an offshore branch over the shelf edge with relatively warm temperatures [e.g., *Fratantoni*, 2001; *Cuny et al.*, 2002]. This offshore flow of relatively warm water into the Labrador Sea consists of Irminger Sea Water that has its origin in waters of the North Atlantic Current (NAC). It follows the cyclonic pathways of the boundary currents within the Labrador Sea [*Marshall and Schott*, 1999]. Recently, evidence for an anticyclonic recirculation offshore of the cyclonic boundary current system has been presented through which warmer and saltier water from the NAC is carried into the Labrador Sea [*Lavender et al.*, 2000; *Fischer and Schott*, 2002; *Fischer et al.*, 2004]. This process may contribute a previously unknown mechanism by which the stratification of the Labrador Sea is maintained and reestablished after a convection winter. In addition to the boundary currents, a slow crossover flow that connects Greenland and Labrador across the deep Labrador Sea was observed in surface drifter and profiling float data [*Cuny et al.*, 2002].

[3] During the winter season, strong buoyancy loss associated with the meteorological conditions causes deep

0148-0227/04/2002JC001551$09.00

convection in the Labrador Sea that can reach depths greater than 2000 m [*Lazier*, 1973, 1988]. In recent years, strong interannual variability of convection intensity has been observed. Intense convection was observed from hydrographic sections across the central Labrador Sea in the early 1990s followed by a multiyear restratification [*Lazier et al.*, 2002]. During the latter phase moored observations showed only weak or moderate convection. In fact, the convection that was observed for the winters 1996 to 1999 (i.e., the winters 1995/1996 to 1998/1999) reached only maximum mixed layer depths of about 1500 m [*Pickart et al.*, 2002; *Lilly et al.*, 2003] and was thus not able to significantly renew the deeper LSW. This moderate convection persisted at least until the winter 2001 and led to the formation of a shallow convective water mass, the upper LSW, that increasingly filled the upper levels of the central Labrador Sea (L. Stramma et al., Deep water changes at the western boundary of the subpolar North Atlantic during 1996 to 2001, submitted to *Deep-Sea Research*, 2003, hereinafter referred to as Stramma et al., submitted manuscript, 2003). The interannual variability in the convection depth was not explainable in terms of the winter to winter variability of the local air-sea fluxes alone. Instead lateral fluxes transporting heat and salt from the boundaries into the central Labrador Sea are needed [*Lazier et al.*, 2002]. In this exchange, mesoscale eddies are presumed to play an essential role. However, first estimates obtained from satellite altimetry indicate that only 25% to 30% of the needed lateral fluxes are carried by the observed eddies [*Lilly et al.*, 2003]. There are at least two possible mechanisms by which eddies may be generated in the Labrador Sea: first mesoscale eddies can be generated by the collapse of the convective regime at the end of the convective season [*Jones and Marshall*, 1993; *Marshall and Schott*, 1999; *Khatiwala and Visbeck*, 2000; *Lilly and Rhines*, 2002] and second by the instability of the boundary current system [*Heywood et al.*, 1994; *White and Heywood*, 1995; *Han and Ikeda*, 1996]. The second mechanism seems to be dominant in the Labrador Sea. *Lilly et al.* [2003], by analyzing TOPEX/Poseidon (T/P) altimeter and in situ data, showed a periodic generation of coherent eddies in the WGC that propagate into the central Labrador Sea. *Prater* [2002], analyzing different data sets, suggested that the seasonal variability of the eddy kinetic energy (EKE) is primarily caused by seasonal variations of the strength and stability of the WGC. Besides the variability of the density field, the variability of the wind curl field is known to be able to change the strength of the WGC. *Greatbatch and Goulding* [1989] found a barotropic response of the WGC to a seasonally varying wind curl, while *Spall and Pickart* [2003] suggested also a baroclinic response of the circulation to variations in the wind stress curl but mainly on longer timescales. *Eden and Böning* [2002], using a general circulation model, showed that the main source of the simulated EKE in the Labrador Sea is barotropic instability of the WGC.

[4] In this presentation we derive EKE fields from T/P and ERS satellite altimeter data that are corrected with respect to their dependence on the significant wave height (SWH). Using corrected EKE fields, we then focus on its temporal and spatial variability in the subpolar North Atlantic and the Labrador Sea. We thus expand on previous work by *Heywood et al.* [1994], *White and Heywood* [1995], *Han and Ikeda* [1996], *Prater* [2002], *Lilly et al.* [2003], and others using earlier satellite altimetry observations of Geosat and/or T/P. The paper is organized as follows. Section 2 describes the data processing and methods. In section 3 the mean EKE field and its annual cycle are discussed. Section 4 concerns the interannual variability, and finally, in section 5 the results are summarized and discussed.

2. Sea Level Anomalies From Altimetry: Available Data and Processing

[5] The altimeter data used are the T/P along-track sea level anomaly (SLA) data from January 1993 to December 2001, provided by Physical Oceanography, Distributed Active Archive Center, Jet Propulsion Laboratory (PO.DAAC) and the ERS-2 along-track SLA data from January 1997 to December 2001, provided by CLS Space Oceanographic Division. The SLA data are corrected for geophysical, tidal, sea state and instrumental effects as well as for orbit errors. The region of interest covers the subpolar North Atlantic and the Labrador Sea between 48° and 65°N and between 62° and 20°W. The global coverage of the T/P satellite consists of 127 ascending/descending tracks during a time of 9.92 days. The ERS-2 satellite has 501 ascending/descending tracks leading to a higher across-track resolution but a larger repetition period of 35 days. The available T/P data have an along-track grid size between 5.7 and 6.2 km and the ERS-2 data a grid size of 6.6 km.

[6] The high noise level inherent in the SLA data requires a preprocessing of the along-track data to obtain relevant parameters describing the mesoscale eddy field in the ocean. The first step in the preprocessing is the elimination of anomalous SLA data for which we used a gradient criterion. After several tests, we decided to remove data points with an along-track SLA gradient larger than 2.5 cm km^{-1}. When using a smaller gradient criterion the strongly increased data loss is not acceptable, a larger criterion instead leads to noisy long-term mean fields that seem not to be realistic.

[7] To reduce the altimeter noise further we applied a Hamming low-pass filter to the along-track data with a cutoff filter wavelength of three along-track grid points. While a three-point filter corresponds to a filter wavelength of 19.8 km for ERS-2 data, for T/P data it corresponds to filter wavelengths between 17.1 and 18.6 km. However, for both products we will use always the same filter, defined by the number of along-track grid points. The use of an along-track filter requires continuous sets of data points with a length of at least three times the filter wavelength of the Hamming filter, i.e., 10 along-track grid points. While due to the gradient criterion of 2.5 cm km^{-1} alone 0.74% of the SLA data are discarded, together with the segment length criterion, they lead to a total data loss of 1.5%.

[8] From the filtered SLA data, cross-track geostrophic velocity anomalies v_c are calculated as follows:

$$v_c = \frac{g}{f}\frac{d\eta}{ds}, \tag{1}$$

where η is the filtered SLA, s is the along-track distance, g is the gravitational constant, and f is the Coriolis parameter.

Table 1. List of Instrumentation Used to Obtain the Eddy Kinetic Energy Time Series in the Central Labrador Sea[a]

Name	Latitude, °N	Longitude, °W	ADCP	Instrument Depth, m	Record Period	
					Start	End
K1	56.56	52.658	up	487	10 Aug. 1996	25 May 1997
K11	56.56	52.658	down	192	23 July 1997	10 July 1998
K21	56.56	52.658	down	200	6 Aug. 1998	18 July 1999
K31	56.56	52.658	up	298	24 July 1999	25 May 2000
K41	56.565	52.675	up	293	3 June 2000	5 June 2001
K51	56.558	52.658	up	297	14 June 2001	24 May 2002

[a]See Figure 1. The table gives the name of the moorings, their location, the kind of the ADCP (upward or downward looking ADCP), its nominal depth, and the data record period. ADCP, acoustic Doppler current profiler.

Assuming the velocity variability to be isotropic, the (geostrophic) EKE is given by

$$\mathrm{EKE} = \overline{\frac{1}{2}\left(v_c^2 + v_a^2\right)} = \overline{v_c^2}, \tag{2}$$

where v_a is the along track velocity and overbars denote time averages [see, e.g., *Stammer*, 1997; *Stammer and Wunsch*, 1999]. Only observations from locations with water depths greater than 900 m were used to avoid unrealistically high EKE values that are artifacts of altimeter data processing over shelf areas.

[9] For each month, the EKE determined at each along-track grid point from the merged T/P and ERS data set is mapped onto a 0.2° longitude × 0.2° latitude horizontal grid using Gaussian weighting functions with a horizontal half-width scale of 50 km and a cutoff scale of 78 km.

[10] The noise inherent in the SLA data led to increased EKE levels. As expected from theoretical considerations [*Chelton et al.*, 2001] parts of the noise is induced by the sea surface roughness due to wind waves and/or swell. To calculate a correction of the obtained EKE fields with respect to the SWH, we used the SWH that is part of the along-track T/P data product provided by NASA. The SWH along the ERS-2 tracks was provided instead by CCAR (Colorado Center for Astrodynamics Research). The SWH of merged T/P and ERS data is mapped for each month between 1997 and 2001 in the same way as we did for the SLA data. A first guess quadratic dependence of the EKE on the SWH is obtained by choosing an area that is characterized by relatively weak drifter-estimated EKE [*Fratantoni*, 2001], i.e., between 54°N and 64°N as well as 27°W and 37°W. When treating larger ranges in latitude one has to consider that f is not constant. Thus we calculated the quadratic dependence of EKE × f^2 on the SWH. The coefficients of the quadratic fit EKE × $f^2 = c_1\overline{\mathrm{SWH}}^2 + c_2\overline{\mathrm{SWH}} + c_3$ are then used to obtain corrected EKE values in the whole subpolar North Atlantic as follows:

$$\mathrm{EKE}_c = 1/f^2\left[g^2\overline{\left(\frac{d\eta}{ds}\right)^2} - c_1\overline{\mathrm{SWH}}^2 - c_2\overline{\mathrm{SWH}}\right]. \tag{3}$$

Using the first guess-corrected EKE, a new region for the estimation of the quadratic dependence was defined. The criterion for a certain grid point to be part of the region is that the mean first guess-corrected EKE and the standard deviation of its 60 month time series being less than 200 and 100 $\mathrm{cm^2 s^{-2}}$ respectively. The obtained region covers about 15% of the whole subpolar North Atlantic. In such a region a large part of the uncorrected EKE should be induced by the noise due to wind waves and/or swell and not by the variability of the eddy field itself. The obtained dependence is used in the following to correct the altimetric estimated EKE field for each month and at each grid point of the 0.2° latitude × 0.2° longitude grid.

[11] To quantify the improvement of the applied correction, we will compare the altimetric EKE with the EKE calculated from moored velocity measurements. Here we use data obtained by acoustic Doppler current profilers during 1996–2002 at the mooring K1 located approximately at 56°35′N and 52°40′W (see Table 1), from which *Lilly et al.* [2003] analyzed a subset from 1996–1999. We vertically averaged the velocity data over three bins having a bin length of 17.4 m. The depth of the central bin was always about 250 m. The EKE time series of the moored observations are then calculated as follows: after subtracting the total mean, the velocity data are 2 day low-pass filtered to remove tides. The EKE is calculated by EKE = $(\overline{u^2 + v^2})/2$, where u and v are the zonal and meridional velocity components and the overbar denotes monthly averages. While the seasonal and interannual variability in the central Labrador Sea will be discussed in section 3, we want to discuss here briefly the differences between the EKE derived from altimetry and from moored observations. The uncorrected altimetric EKE shows several large peaks that are not visible in the moored EKE (Figure 1). These peaks that are occurring mainly during December/January, when the SWH in that region is maximum, are strongly reduced after applying the correction. By calculating the correlation between the altimetric EKE and the moored EKE, we obtained correlation coefficients of 0.46 as well as 0.77 for the correlation between uncorrected altimetric EKE and moored EKE as well as corrected altimetric EKE and moored EKE respectively. Owing to the different temporal and spatial sampling of both techniques, the missing centrifugal acceleration term in the altimetrically estimated EKE as well as due to the different oceanic and/or measurement noise inherent in the data, a perfect correlation between altimetric and moored EKE cannot be expected. However, from the presented comparison we conclude that, at least in the central Labrador Sea, the applied correction with respect to the SWH significantly improves the altimetrically estimated EKE.

[12] It should be noted at the outset that while the altimetry analysis will give useful information on regional, seasonal and interannual aspects of the eddy field, it is also clear that particularly small and weak eddies may be lost in the altimetry noise. By analyzing mooring data from the central Labrador Sea, *Lilly et al.* [2003] also identified

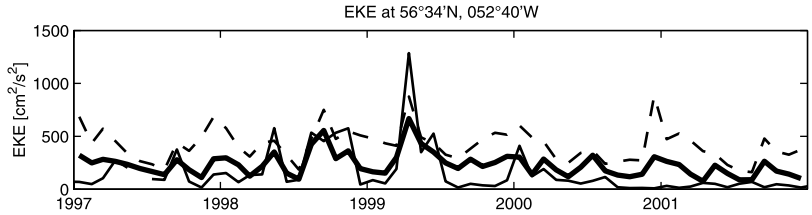

Figure 1. Time series of monthly mean eddy kinetic energy (EKE) at the mooring position K1 at 56°34′N, 52°40′W as obtained from velocity measurements at ~250 m water depth (thin solid line), from altimetric observation with (thick solid line) and without (dashed line) a correction with respect to significant wave height (SWH).

eddies with radii as small as 5 km. Clearly, such eddies cannot be resolved by applying the above mentioned cutoff filter wavelengths.

3. EKE Field and Its Annual Cycle

[13] The mean EKE field from merged T/P and ERS altimeter data averaged over the 5 year period 1997–2001 is shown in Figure 2. The mean EKE field is in general agreement with results previously obtained [e.g., *Fratantoni*, 2001; *Reverdin et al.*, 2003; *Lilly et al.*, 2003]. It shows higher levels associated with the main currents in the region: The most prominent feature in the mean EKE field is the *Northwest Corner* of the NAC east of Newfoundland. The maximum mean EKE value in this region of about 1400 cm^2s^{-2} as well as regions of increased EKE east and west of the Reykjanes Ridge agrees well with the results obtained from surface drifter data [*Fratantoni*, 2001; *Reverdin et al.*, 2003]. In the Labrador Sea, there is a conspicuous permanent EKE maximum off southwest Greenland as well as a band of increased EKE along the LC in the southern Labrador Sea as it was very similarly found by *Lilly et al.* [2003], who studied T/P data of the period 1994–2000. *Prater* [2002] analyzed the standard deviation of T/P SLA and found besides the peak off southwest Greenland a peak in the central Labrador Sea at 58°N, 52°W. This peak can also be found in the presented EKE distribution but having only about 100 cm^2s^{-2} higher levels then the background noise.

[14] Amplitude, phase, and explained variance of the annual harmonic as calculated from 5 year merged T/P and ERS altimeter data are shown in Figure 3. The amplitude of the annual harmonic of the EKE is characterized by larger values in the area of the Northwest Corner, the LC, and the WGC. Only in the last two regions the annual harmonic explains a large part of the total variance of the EKE. The annual cycle of the WGC EKE was described in detail by *Lilly et al.* [2003]. According to their analysis, the mean annual cycle of the WGC EKE peaks in January and the EKE maximum propagates southward during January/March with about 5 cm s^{-1}. In addition, they found the pathways for several strong anticyclonic eddies from their origin in the WGC to the central Labrador Sea, where these eddies were finally observed in mooring data.

[15] Recent results by *Eden and Böning* [2002] with the GFDL-MOM/FLAME eddy resolving high-resolution model (1/12° horizontal resolution and 45 vertical levels) forced by monthly averaged winds show good agreement with the EKE pattern just presented. Particularly evident is the permanent EKE maximum southwest of Greenland, which is enhanced in winter. The authors find that the change of topographic slope which steepens considerably west of Cape Farewell leads to a narrowing and acceleration of the WGC profile and its partial detachment from the topography. In this transition region the current becomes unstable, causing the regional EKE maximum. Analyzing the instability terms the authors further conclude that the barotropic instability term is the dominant energy source for the EKE.

[16] The barotropic instability also explains the seasonal EKE cycle in the WGC region in the model simulation, and is itself a consequence of the seasonal variation of the WGC strength. The main reason for the seasonal cycle of the WGC seems to be the seasonal cycle of basin-wide wind stress curl. In fact, 2 year moored measurements within the LC at 53°N at the southern boundary of the subpolar gyre revealed a seasonal cycle characterized by an increase of the boundary current flow from April to February followed by a rather sudden decrease of the flow by the end of the winter [*Fischer et al.*, 2004]. The observed seasonal cycle agrees quite well with results obtained by *Greatbatch and Goulding* [1989] who simulated seasonal transport fluctuations in the subpolar gyre with a barotropic model of the North Atlantic driven by seasonally varying wind stress

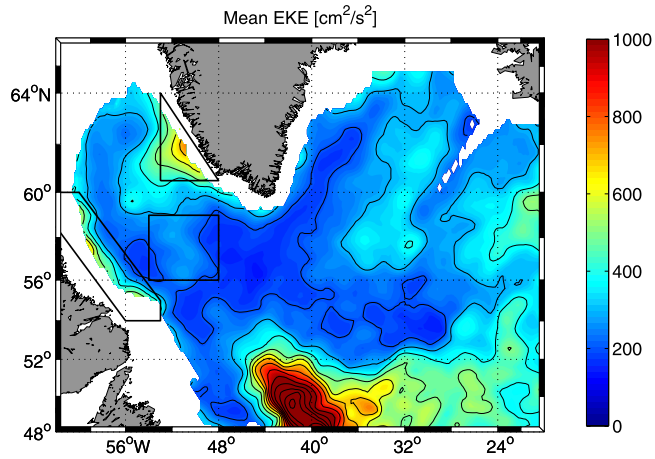

Figure 2. Mean EKE distribution ($cm^2\ s^{-2}$) from merged TOPEX/Poseidon (T/P) and ERS data for the period 1997–2001. The spacing of the contour levels is 100 $cm^2\ s^{-2}$. Also included are three boxes that represent the West Greenland Current (WGC) region, the central Labrador Sea, and the Labrador Current (LC) region.

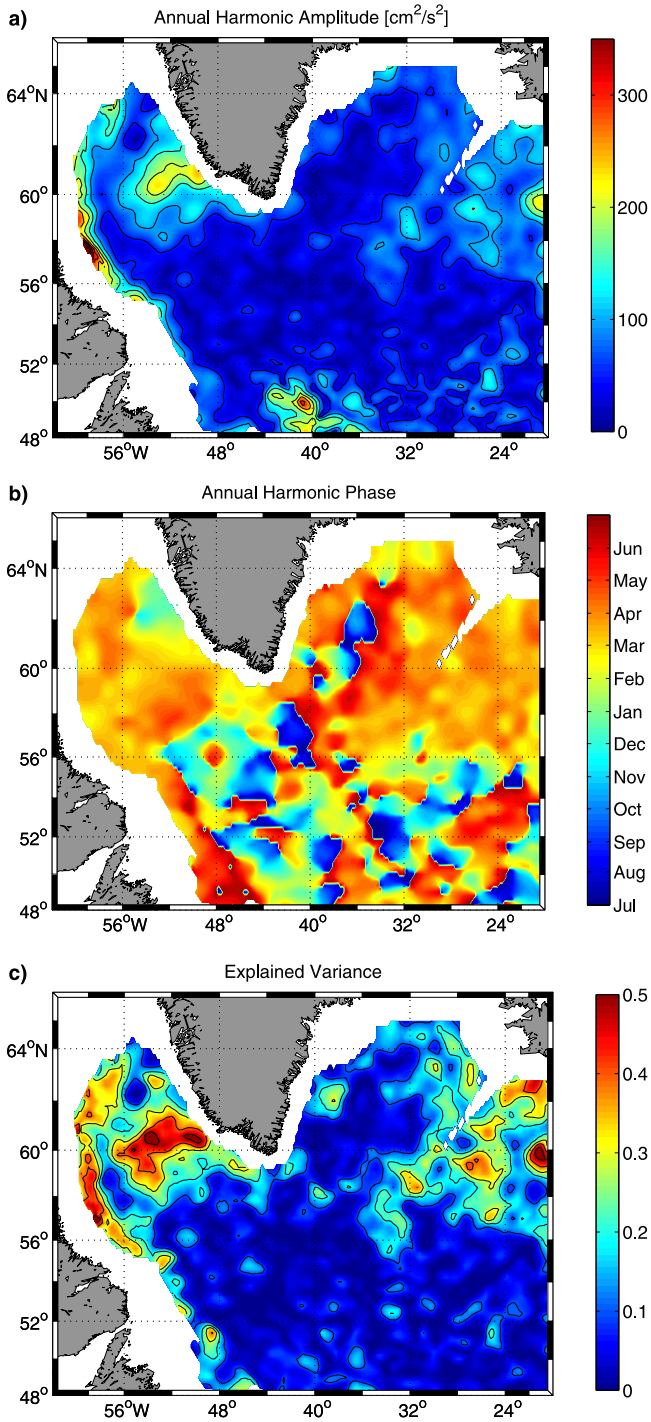

Figure 3. (a) Amplitude (cm^2 s^{-2}), (b) phase (month of maximum EKE), and (c) explained variance of the annual harmonic of the EKE from merged T/P and ERS data for the period 1997–2001.

fields. They found maximum gyre transports in January and February with an adjustment time smaller than 1 month.

[17] Figure 4 shows the mean wind stress curl as well as amplitude and phase of the annual harmonic as calculated from National Centers for Environmental Prediction wind stress data for the same period as the EKE was calculated. A strong amplitude of the annual harmonic can be observed east and west of Greenland with maximum cyclonic wind stress curl during January. However, the annual EKE harmonic in the WGC region peaks during January/February (Figure 3), i.e., there is only a small phase lag between maximum wind stress curl and maximum EKE. Such fast

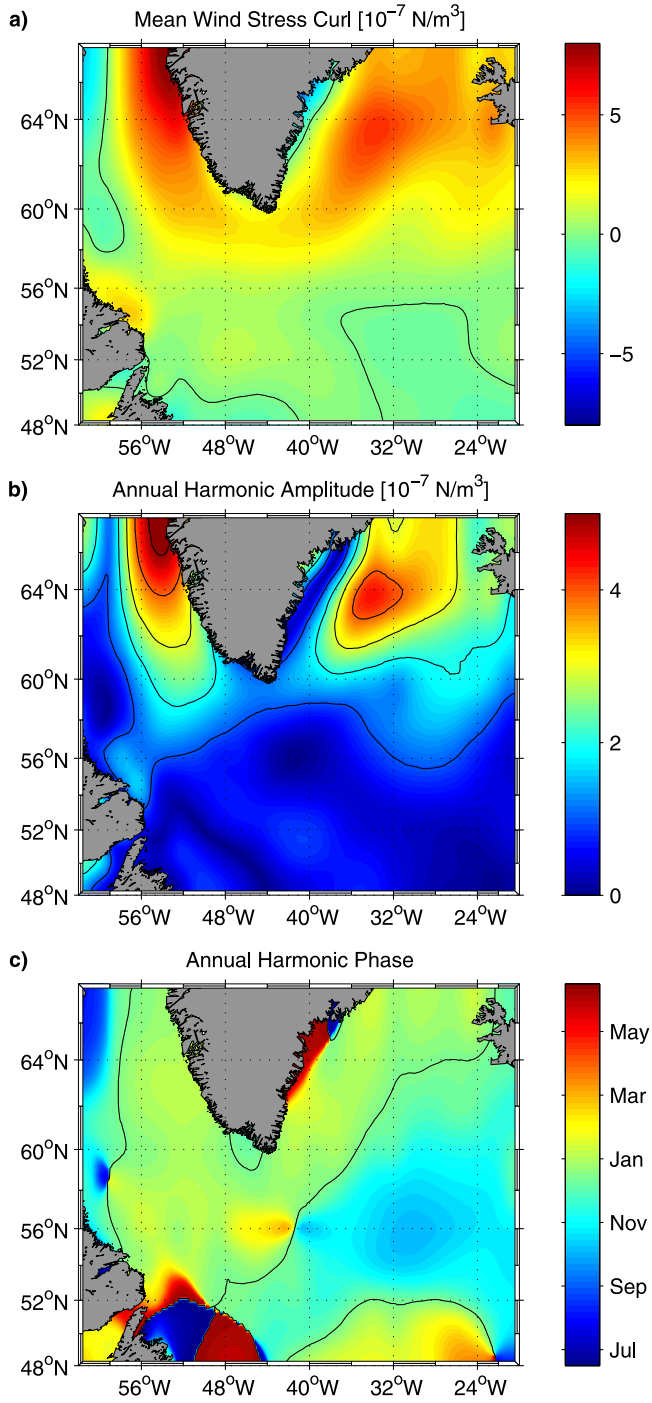

Figure 4. (a) Mean wind stress curl distribution (N m^{-3}), (b) amplitude (N m^{-3}), and (c) phase (month of maximum cyclonic wind stress curl) of the annual harmonic of wind stress curl from National Centers for Environmental Prediction data for the period 1996–2000. The contour levels mark zero wind stress curl in Figure 4a, are spaced by 10^{-7} N m^{-3} in Figure 4b, and mark 1 January in Figure 4c.

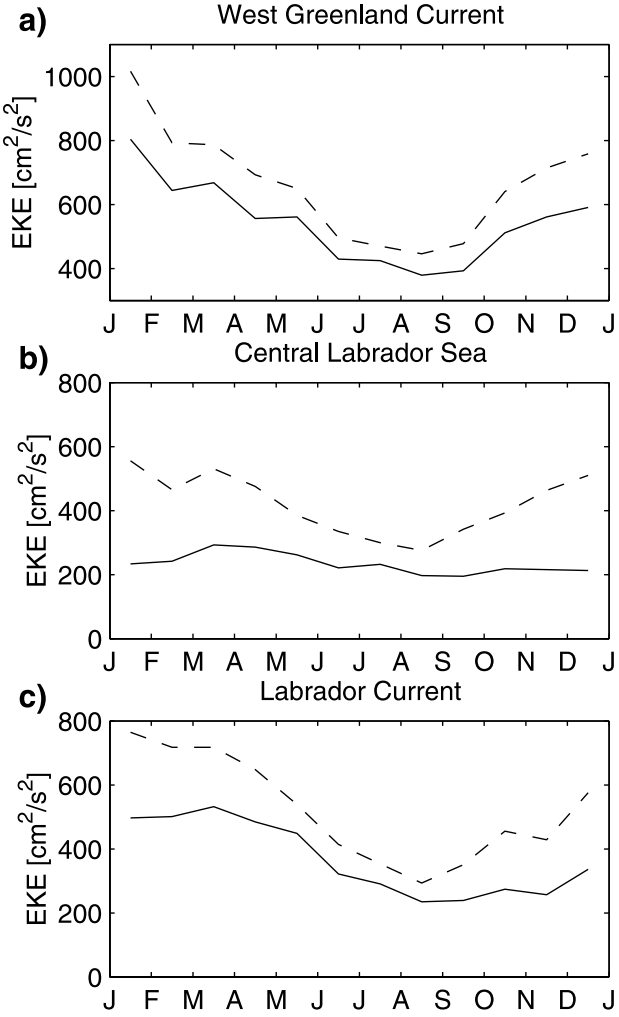

Figure 5. Mean annual cycle of EKE averaged for (a) the WGC region, (b) the central Labrador Sea, and (c) the LC region from merged T/P and ERS data for the period 1997–2001. Dashed lines denote uncorrected EKE values, and solid lines denote EKE values that are corrected with respect to SWH. The three boxes are marked in Figure 2.

response of the WGC EKE to changes in the strength of the WGC was also found in the numerical study of *Eden and Böning* [2002] discussed above.

[18] Besides the southward propagation of WGC EKE, parts of the WGC EKE also propagate westward as well as northward within the boundary current (Figure 3). However, the amplitude of the LC EKE annual harmonic has maximum values between 56° and 60°N along the shelf edge off Labrador and is very likely generated locally, possibly by the instability of the LC itself. The LC EKE north of 56°N peaks in February/March. Farther south the amplitude of the annual harmonic of LC EKE becomes smaller and it peaks later in the year. The influence of the LC EKE on the eddy field in the central Labrador Sea seems to be much weaker than that of the WGC EKE as the mean LC EKE and the amplitude of its annual harmonic are well separated from the central Labrador Sea by local minima. However, *Cuny et al.* [2002] analyzed surface drifter trajectories as well as profiling float data and found several pathways from Greenland to Labrador across the central Labrador Sea indicating a direct water exchange between the central Labrador Sea and the LC. By analyzing surface drifter data, *Reverdin et al.* [2003] found two kinds of drifter pathways, first those that loop across the central Labrador Sea within eddies, and second pathways that, after following the LC, leave the boundary current toward the interior of the Labrador Sea, in particular near 53°N.

[19] The mean annual cycles of the uncorrected and corrected EKE averaged in different regions of the Labrador Sea are shown in Figure 5. There are large differences in magnitude and structure between both curves. The correction in the WGC region merely leads to a shift in the magnitude of the EKE, in the central Labrador Sea as well as in the LC region it leads moreover to a shift in the month of maximum EKE. As discussed in section 2, the strong maximum in the annual cycle of the uncorrected EKE in December/January in the central Labrador Sea resulting from the SWH peak during December/January and therefore is missing in the corrected EKE.

4. Interannual Variability

[20] EKE time series of the WGC region (60.5°–64°N, 48°–53°W) and of the central Labrador Sea (56°–59°N, 48°–53°W, used boxes see also Figure 2) are calculated by spatial averaging gridded monthly EKE values (Figure 6). The complete time series from 1993–2001 is calculated using T/P data alone. In general, there is good agreement of the time series 1997–2001 from merged T/P and ERS data with T/P data alone. While the variability agrees quite well, there seems to be a slight mean offset in the central Labrador Sea between merged data and T/P data alone that possibly results from differences in the statistical dependence of the EKE on the SWH. For the description of the interannual variability of the eddy field we will use the time series calculated from T/P data alone.

[21] The EKE in the WGC is on average more than 300 cm^2s^{-2} higher than in the central Labrador Sea (Figure 6). Besides the seasonal variability discussed in section 3, the time series show strong interannual variability. The early winter maxima of the WGC EKE are largest during 1993 as well as 1997 to 1999. The maximum annual average of the EKE is found in the year beginning in summer 1996, while local minima are found during 1994 and 2000. The interannual variability in the central Labrador Sea is quite different from that in the WGC region. In the central Labrador Sea, peaks of maximum EKE are obtained during March/April 1993–1997, except 1996. The strong peak during 1999 at mooring K1 at 56°34′N, 52°40′W (Figure 1) is only associated with slightly enhanced EKE in the box average of the central Labrador Sea over a generally increased background EKE level.

[22] A latitude-time diagram of the EKE in the Labrador Sea averaged between 48°W and 54°W is shown in Figure 7 obtained by using merged T/P and ERS data from the period 1997–2001. When using T/P data alone, only slight differences occur during that period (compare Figures 7 and 8a). *Lilly et al.* [2003] showing a similar plot for the mean annual cycle estimated a mean southward propagation speed of the WGC EKE into the central Labrador Sea of

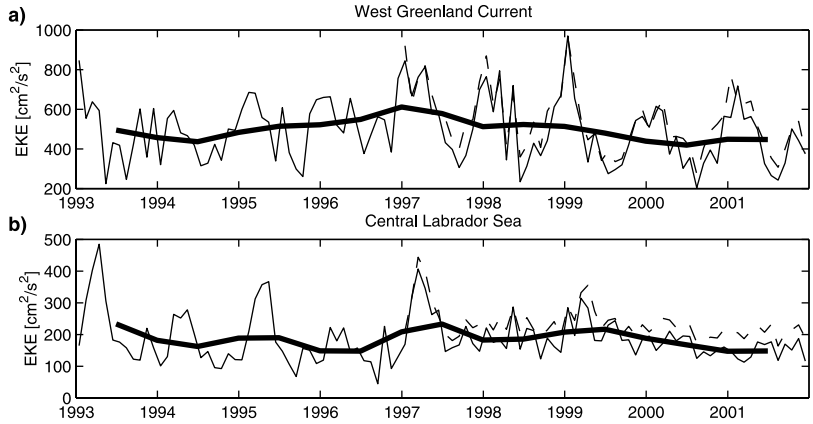

Figure 6. Time series of EKE averaged for (a) the WGC region and (b) the central Labrador Sea from merged T/P and ERS data for the period 1997–2001 (dashed line) and from T/P data alone for the period 1993–2001 (thin solid line). Also included are 6 month overlapping annual averages (thick solid line) of T/P data alone. The two boxes are marked in Figure 2.

4.7 cm s^{-1}. For each year from 1997 to 2001, the propagation line corresponding to that speed is included in Figure 7 and indicates that the southward propagation obtained here has in general a smaller propagation speed than that estimated by *Lilly et al.* [2003] for the period 1994–2000.

[23] In the following we want to focus on an aspect of the interannual variability of the EKE field in the Labrador Sea that is related to changes in the amplitude of the annual cycle. From the nine year-long time series of the EKE (Figure 7) time series of the amplitude (Figure 8b) and phase (Figure 8c) of the annual harmonic of 2-year-long segments are calculated as function of latitude and time. The explained variance (Figure 8d) gives the part of the total variance of the 2 year segments that is explained by the annual harmonic.

[24] The amplitude of the annual harmonic of the WGC EKE was small during a first period between 1994–1996 with maximum amplitudes of about 150 cm^2s^{-2} compared to a second period between 1997–2000 when it reached values up to 250 cm^2s^{-2}. In addition, the annual harmonic of the WGC EKE north of 61°N between 1994–1996 explains only a small part of the total variance within the 2 year segments used for the fit (Figure 8d). From Figure 8a it becomes evident that most of the total variance during that time is associated with shorter period fluctuation than the annual period. This behavior suggests a more continuous WGC EKE generation during 1994–1996 compared to alternating low summer and high winter EKE levels during 1997–2000. During the second period the phase of the annual harmonic north of 61°N is well defined as it explains a large part of the total variance and maximum WGC EKE is found during January (Figure 8c). This timing corresponds well with the above discussed mechanism of eddy generation due to the seasonally varying strength of the WGC that is forced by the seasonal peak in the wind curl field (see Figure 4).

[25] In the central Labrador Sea the annual harmonic of EKE has larger amplitudes between 1994–1996 than between 1997–2000 (Figure 8b). The strong annual cycle in the first period results not only from large EKE maxima during March/April but also from the particularly low summer EKE (Figure 6b). This behavior corresponds to a rapid destruction of the EKE generated during winter in the central Labrador Sea during 1994–1996. During 1997–2000, instead, the EKE changes only slightly around an generally enhanced mean EKE level corresponding to the

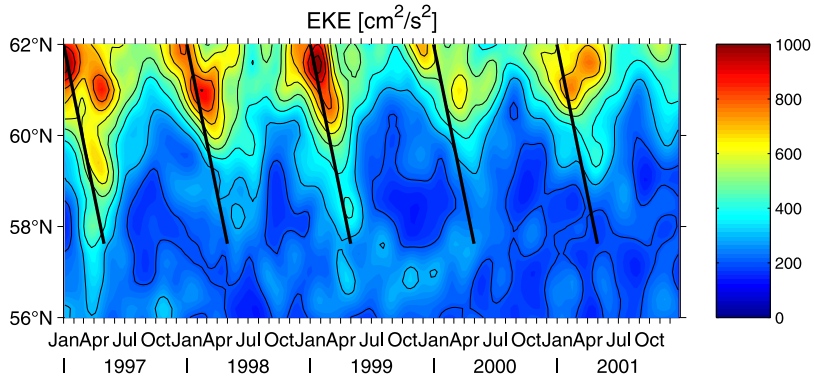

Figure 7. Latitude-time diagram of the EKE in the Labrador Sea averaged between 48° and 54°W from merged T/P and ERS data for the period 1997–2001. The solid black lines mark a southward propagation speed of 4.7 cm s^{-1}.

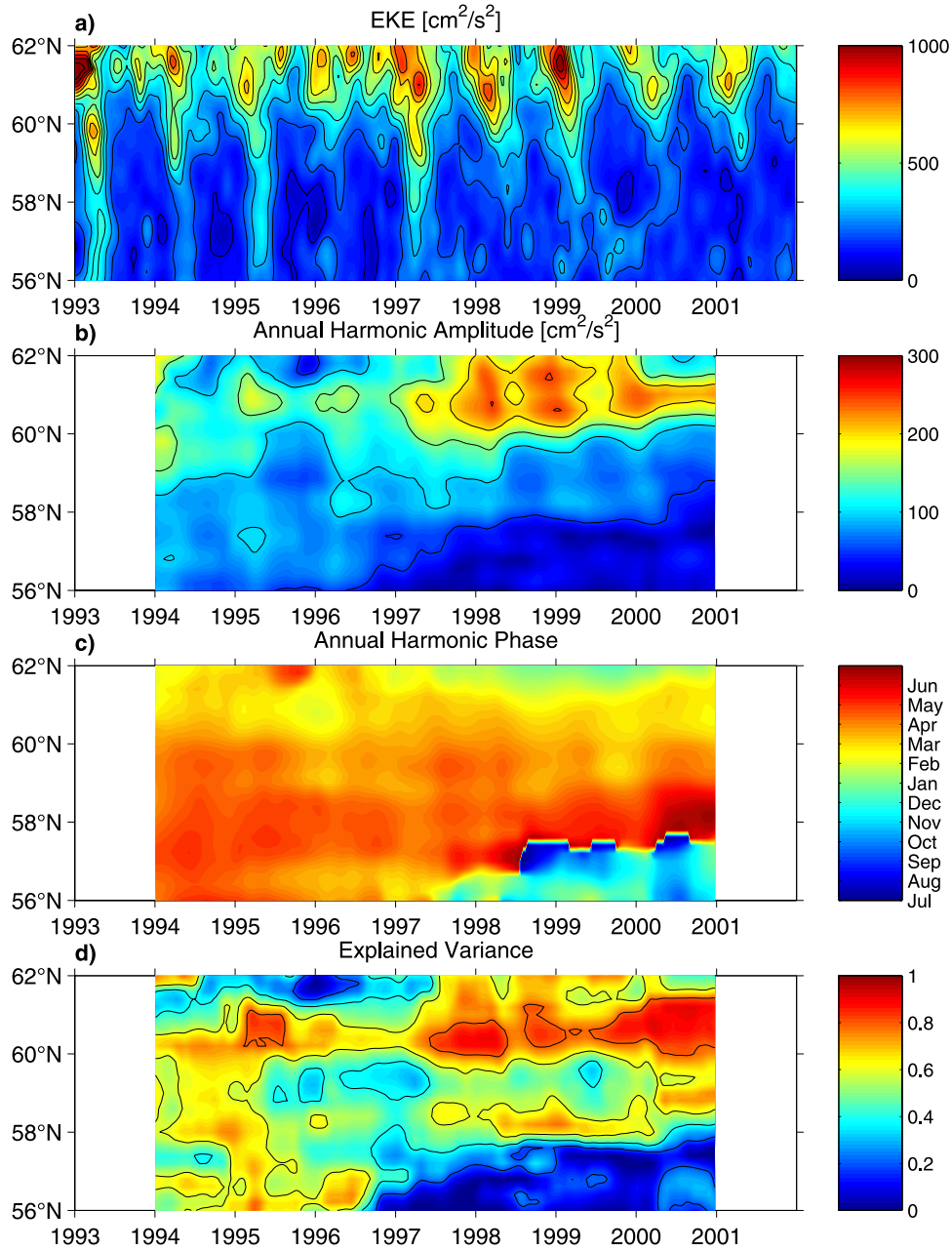

Figure 8. Latitude-time diagram of the EKE in the Labrador Sea averaged between 48° and 54°W from T/P data alone for the period 1993–2001 (Figure 8a) as well as amplitude (cm^2 s^{-2}), phase (month of maximum EKE), and explained variance of the annual harmonic of the EKE as calculated from 2-year-long segments. Note the almost instantaneous generation of EKE in the central Labrador Sea (between 56°N and 59°N) during April/March 1993–1997, except 1996 combined with its fast destruction during the summer 1993–1995 and the maintenance of increased EKE levels in the central Labrador Sea during 1997–2000.

maintenance of the winterly generated EKE until the following winter.

[26] The distribution of the phase of the annual harmonic shows significant differences in the propagation characteristics of the Labrador Sea EKE between the two periods. During the first period 1994–1996 the phase of the annual harmonic in the central Labrador Sea between 56°N and 60°N is almost constant with maximum EKE in March/April (Figure 8c). Note that this statement is also valid for 1993 (compare Figure 8a). This behavior indicates either a very fast propagation or, more likely, an almost simultaneous generation of EKE in the central Labrador Sea. During the second period 1997–2000 the southward propagation from the WGC at 62°N into the central Labrador Sea is much more evident. On the basis of a mean phase difference of about 6 months between 62°N and 58°N (Figure 8c), a southward propagation speed of about 3 cm s^{-1} results. The year 1997 that is characterized by the peak in the interannual variability of Labrador Sea EKE seems to be a transition period: On the one hand there is a strong

EKE maximum in January near 62°N propagating southward, away from the northern boundary, on the other hand there is an almost simultaneously increase of the EKE in the central Labrador Sea between 56°N and 60°N during March/April (see also Figure 7).

[27] The analysis of eddy features in moored current meter data by *Lilly et al.* [2003] revealed the existence of ''convective lenses'' with middepth-intensified currents predominantly during the first period. From the θ/*S* properties of the observed eddies the authors identified them as originating in the central Labrador Sea during deep convection. Moreover, the mooring results showed that after mid-1997 a second type of eddies occurs with surface intensified currents and larger radii than the ''convective lenses.'' The authors identified them as predominantly buoyant, long-lived anticyclones originating in the WGC EKE maximum. Implications of the comparison between results obtained from the moored observation with the results obtained in the present study will be discussed in section 5.

5. Summary and Discussion

[28] In this paper we have presented an analysis of the temporal and spatial variability of the EKE field as derived from T/P and ERS altimeter data from the subpolar North Atlantic and the Labrador Sea. The T/P data cover a period from 1993 to 2001 and the ERS data from 1997 to 2001. The derivation of EKE fields from altimetric derived SLA data requires a careful preprocessing of the available along-track data. Prior to the calculation of along-track SLA gradients, anomalous SLA data has to be removed and the along-track SLA data has to be filtered in space to reduce the noise inherent in the SLA data. A close examination of the noise showed a statistical relationship between the calculated EKE and the SWH that is simultaneously measured by the altimeter aboard the T/P and ERS satellites. Here, we used a quadratic correction of the calculated EKE with respect to the SWH that is necessary when the seasonal or interannual variability of the EKE has to be explored as otherwise temporal and spatial variations of the SWH could strongly affect the obtained results. A comparison between EKE time series calculated from moored and altimetric observations shows a significant increase of their correlation after applying the correction. The correction particularly affects the annual cycle of the central Labrador Sea EKE: The strong maximum in the annual cycle of the uncorrected EKE field during December/January results from the seasonal SWH maximum and is missing in the corrected EKE field.

[29] The corrected EKE fields are then used to describe the mean as well as the seasonal and interannual variability of the EKE in the subpolar North Atlantic. The mean EKE field agrees well with recent results obtained by drifter data [*Fratantoni*, 2001] or T/P data [*Lilly et al.*, 2003]. Recently, the eddy field in this region as well as its role in the larger-scale circulation was studied in great detail by *Lilly et al.* [2003] using as major data source current meter moorings and satellite altimetry. The sharpened view on the altimetrically observed EKE variability obtained here mainly results from the improved treatment of noise inherent in the data as well as from the inclusion of ERS altimeter data in the analysis having a better spatial resolution.

[30] In the mean EKE field that is obtained from a merged T/P and ERS data set for the period from 1997 to 2001 particularly high EKE values were found in the WGC region southwest of Greenland as well as in LC region along the shelf edge off Labrador. The calculation of the annual harmonic of the EKE for the same period reveals a large seasonal variability in both regions. However, while the LC EKE maximum and the maximum of its annual cycle are well separated from the central Labrador Sea by local minima suggesting a small influence of the LC EKE on the EKE level of the central Labrador Sea, the annual harmonic clearly indicates a propagation of EKE from the WGC region into the central Labrador Sea.

[31] During the time of altimetric observations strong interannual variability in the EKE fields occurred. In the WGC region increased EKE levels were found during early winters of 1993 and 1997–1999. The evolution of the EKE in the central Labrador Sea is quite different from that in the WGC. Here maxima in the EKE levels were found during March/April of 1993, 1995, 1997, and with somewhat smaller amplitude 1994. However, possibly the most important result of this study is the detailed view on the space-time evolution of the EKE in the Labrador Sea during different winters between 1993 and 2001 (Figures 7 and 8). From 1994–1996 the annual cycle in the WGC north of 61°N was weak. Nevertheless, there were considerably high EKE levels throughout the whole period indicating a more continuous generation of EKE in the WGC. These years were characterized by the presence of large volumes of deep LSW associated with a doming of the isopycnals in the central Labrador Sea [*Lazier et al.*, 2002]. A possible increase in the horizontal density gradients related to this doming could have led to an increased strength of the WGC and thus to the observed more continuous EKE generation. However, from 1997–2001 we observed a strong annual cycle in the WGC EKE generation, with maximum values during January and particularly strong minima during summer. This period is characterized by the increasing formation of lighter, upper LSW [*Lazier et al.*, 2002; Stramma et al., submitted manuscript, 2003]. In this case the smaller horizontal density gradient could have led to a decreased strength of the WGC and the observed strong annual cycle may be explained by the annual cycle of the wind stress curl forcing the WGC to switch between more stable and unstable phases.

[32] The propagation characteristics of the altimetrically estimated EKE indicates a slow propagation of the WGC EKE into the central Labrador Sea during 1997–2001 with nearly 3 cm s^{-1}. From mooring data, *Lilly et al.* [2003] identified the associated eddies, that occurred in the central Labrador Sea after mid-1997, as predominantly buoyant, long-lived anticyclones transporting warmer and saltier Irminger Sea Water into the central Labrador Sea. This situation is well presented in a recent model study by *Eden and Böning* [2002], who demonstrated the importance of the WGC as eddy shedding regime sending mostly anticyclonic eddies into the central Labrador Sea that are generated by the barotropic instability of the boundary current.

[33] An almost simultaneously increase of the EKE during March/April in the central Labrador Sea between 56°N and 60°N can instead be observed during 1993–1995 and 1997. The 3 years 1993–1995 are characterized by

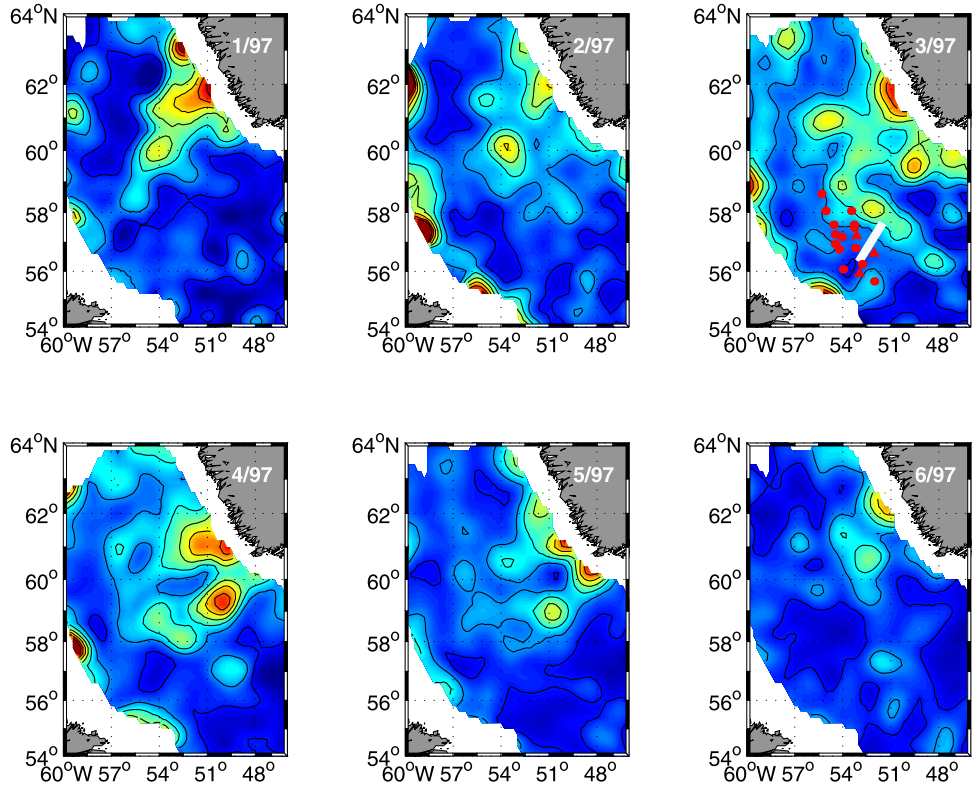

Figure 9. Monthly mean EKE in the Labrador Sea for the period January to June 1997 from merged T/P and ERS data. The contour levels are spaced by 200 $cm^2\ s^{-2}$. In the March 1997 subplot is given the locations of mixed layer depths between 800 and 1000 m (red circles) and between 1000 and 1350 m (red triangles) from profiling floats measurements between November 1996 and April 1997 [*Lavender et al.*, 2002] as well as the location of moderate convection that is determined from a hydrographic section taken during March 1997 as being the region bounded by the outcrop positions of the isopycnal surface σ_θ = 27.75 kg m^{-2} (white bar) [*Pickart et al.*, 2002].

deep convection associated with the renewal of deep LSW [*Lilly et al.*, 2003]. From mooring data, *Lilly et al.* [2003] revealed the existence of short-lived "convective lenses" predominantly during these years that were identified as originating in the central Labrador Sea during deep convection. The observations of short-lived eddies correspond to the rapid destruction of EKE in the central Labrador Sea that is observed in the altimeter data.

[34] The winter 1997 that is characterized by the interannual EKE maximum seems to mark the transition between both states described above. This winter is already covered by ERS altimeter data having a higher spatial resolution than the T/P altimeter data. The use of merged T/P and ERS data thus allow a more detailed description of the evolution of the EKE during that period.

[35] During January 1997 large EKE levels were observed in the WGC region that propagate away from the source region. However, during March 1997 an instantaneous increase of the EKE is observed in the whole central Labrador Sea that cannot be explained by the eddy propagation from the WGC (Figure 7). In particular, during March 1997 a band of enhanced EKE can be identified reaching from 54°W, 59°N to 48°W, 56°N (Figure 9). This band marks the northern boundary of the convective patch as observed during that winter from profiling float data by *Lavender et al.* [2002]. From a hydrographic section taken during March 1997 [*Pickart et al.*, 2002] the extension of the convective patch can be estimated by the outcropping of the isopycnal σ_θ = 27.75 kg m^{-3}, which marks the upper bound of the LSW (white bar in Figure 9). Following the hydrographic section toward north, buoyant water originating in the WGC was observed near the surface that prevents this region from deep convection. However, the region north of the convective patch that is associated with an increased horizontal density gradient coincides with the band of enhanced EKE observed with altimetry. The southern boundary of the convective patch may be the LC that was also associated with an increased EKE level during March 1997. After the fast destruction of the "convective lenses," the remaining EKE during June 1997 may correspond to the long-lived anticyclones observed by *Lilly et al.* [2003] in mooring data that are generated in the WGC region some months before. In spite of strong surface heat fluxes during February/March 1997, the winter 1997 was moderate with respect to atmospheric forcing and resulted in moderate convection reaching down to 1500 m water depth [*Lab Sea Group*, 1998; *Pickart et al.*, 2002]. Nevertheless, the observed behavior of the EKE field during that winter is in general agreement with the scheme given by *Marshall and Schott* [1999], in which the collapse of the convective regime at the end of the convective season is associated with baroclinic instabilities leading to enhanced EKE levels. The

winter 1997 may thus be seen as an exemplar case for the evolution of the EKE that is largely generated near the convective patch in the central Labrador Sea.

[36] **Acknowledgments.** This work was supported by the German Science Foundation (DFG) as part of the "Sonderforschungsbereich" SFB 460 Project: "Dynamics of the Thermohaline Circulation Variability." The TOPEX/Poseidon SLA and SWH altimeter data are supplied by PO.DAAC, the ERS-2 SLA altimeter data are supplied by CLS Space Oceanographic Division, and the ERS-2 SWH altimeter data are supplied by CCAR. We thank P. Gimeno for processing the ERS-2 SWH altimeter data.

References

Chelton, D. B., J. C. Ries, B. J. Haines, L.-L. Fu, and P. S. Callahan (2001), Satellite altimetry, in *Satellite Altimetry and the Earth Sciences*, edited by L.-L. Fu and A. Cazenave, pp. 1–131, Academic, San Diego, Calif.

Cuny, J., P. B. Rhines, P. P. Niiler, and S. Bacon (2002), Labrador Sea boundary currents and the fate of the Irminger Sea Water, *J. Phys. Oceanogr.*, *32*, 627–647.

Eden, C., and C. Böning (2002), Sources of eddy kinetic energy in the Labrador Sea, *J. Phys. Oceanogr.*, *32*, 3346–3363.

Fischer, J., and F. Schott (2002), Labrador Sea Water tracked by profiling floats—From the boundary current into the open North Atlantic, *J. Phys. Oceanogr.*, *32*, 573–584.

Fischer, J., F. A. Schott, and M. Dengler (2004), Boundary circulation at the exit of the Labrador Sea, *J. Phys. Oceanogr.*, in press.

Fratantoni, D. M. (2001), North Atlantic surface circulation during the 1990s observed with satellite-tracked drifters, *J. Geophys. Res.*, *106*, 22,067–22,093.

Greatbatch, R. J., and A. Goulding (1989), Seasonal variations in a linear barotropic model of the North Atlantic driven by the Hellerman and Rosenstein wind stress field, *J. Phys. Oceanogr.*, *19*, 572–595.

Han, G., and M. Ikeda (1996), Basin-scale variability in the Labrador Sea from TOPEX/POSEIDON and Geosat altimeter data, *J. Geophys. Res.*, *101*, 28,325–28,334.

Heywood, K. J., E. L. McDonagh, and M. A. White (1994), Eddy kinetic energy of the North Atlantic subpolar gyre from satellite altimetry, *J. Geophys. Res.*, *99*, 22,525–22,539.

Jones, H., and J. Marshall (1993), Convection with rotation in a neutral ocean: A study of open ocean deep convection, *J. Phys. Oceanogr.*, *23*, 1009–1039.

Khatiwala, S., and M. Visbeck (2000), An estimate of the eddy-induced circulation in the Labrador Sea, *Geophys. Res. Lett.*, *27*, 2277–2280.

Lab Sea Group (1998), The Labrador Sea Deep Convection Experiment, *Bull. Am. Meteorol. Soc.*, *79*, 2033–2058.

Lavender, K. L., R. E. Davis, and W. Brechner Owens (2000), Direct velocity measurements in the Labrador and Irminger Seas describe pathways of Labrador Sea water, *Nature*, *407*, 66–69.

Lavender, K. L., R. E. Davis, and W. Brechner Owens (2002), Observation of open-ocean deep convection in the Labrador Sea from subsurface floats, *J. Phys. Oceanogr.*, *32*, 511–526.

Lazier, J. (1973), The renewal of Labrador Sea Water, *Deep Sea Res.*, *20*, 341–353.

Lazier, J. (1988), Temperature and salinity changes in the deep Labrador Sea, 1962–1986, *Deep Sea Res.*, *35*, 1247–1253.

Lazier, J., R. Hendry, A. Clarke, I. Yashayaev, and P. Rhines (2002), Convection and restratification in the Labrador Sea, 1990–2000, *Deep Sea Res.*, *49*, 1819–1835.

Lilly, J. M., and P. B. Rhines (2002), Coherent eddies in the Labrador Sea observed from a mooring, *J. Phys. Oceanogr.*, *32*, 585–598.

Lilly, J. M., P. B. Rhines, F. Schott, K. Lavender, J. Lazier, U. Send, and E. D'Asaro (2003), Observations of the Labrador Sea eddy field, *Prog. Oceanogr.*, *59*, 75–176.

Marshall, J., and F. Schott (1999), Open-ocean convection: Observations, theory, and models, *Rev. Geophys.*, *37*, 1–64.

Pickart, R. S., D. J. Torres, and R. A. Clarke (2002), Hydrography of the Labrador Sea during active convection, *J. Phys. Oceanogr.*, *32*, 428–457.

Prater, M. (2002), Eddies in the Labrador Sea as observed by profiling RAFOS floats and remote sensing, *J. Phys. Oceanogr.*, *32*, 411–427.

Reverdin, G., P. P. Niiler, and H. Valdimarsson (2003), North Atlantic Ocean surface currents, *J. Geophys. Res.*, *108*(C1), 3002, doi:10.1029/2001JC001020.

Spall, M. A., and R. S. Pickart (2003), Wind-driven recirculations and exchanges in the Labrador and Irminger Seas, *J. Phys. Oceanogr.*, *33*, 1829–1845.

Stammer, D. (1997), Global characteristics of ocean variability estimated from regional TOPEX/POSEIDON altimeter measurements, *J. Phys. Oceanogr.*, *27*, 1743–1769.

Stammer, D., and C. Wunsch (1999), Temporal changes in eddy energy of the oceans, *Deep Sea Res.*, *46*, 77–108.

White, M. A., and K. J. Heywood (1995), Seasonal and interannual changes in the North Atlantic subpolar gyre from Geosat and TOPEX/POSEIDON altimetry, *J. Geophys. Res.*, *100*, 24,931–24,941.

P. Brandt, A. Funk, C. S. Martins, and F. A. Schott, Institut für Meereskunde, Universität Kiel, Düsternbrooker Weg 20, D-24105 Kiel, Germany. (pbrandt@ifm.uni-kiel.de; afunk@ifm.uni-kiel.de; csena@ifm.uni-kiel.de; fschott@ifm.uni-kiel.de)